



Trade Science Inc.

Environmental Science

An Indian Journal

Current Research Paper

ESAIJ, 8(4), 2013 [148-155]

Sulphur-doped titanium dioxide nanoparticles for visible-light induced photo-mineralization of Reactive Red 141

Selma K.Kuriechen¹, Sepperumal Murugesan^{2*}

¹School of Energy, Environment & Natural Resources, Madurai Kamaraj University, Madurai-625 021, (INDIA)

²Dept of Inorganic Chemistry, School of Chemistry, Madurai Kamaraj University, Madurai-625 021, (INDIA)

E-mail : smsan@mail.com

ABSTRACT

Non-metal doped photocatalysts (Sulphur or fluorine-doped TiO₂) prepared through sol-gel technique are characterized using powder X-ray diffraction (XRD) and UV-vis diffuse reflectance spectroscopic techniques. The prepared photocatalysts consist of purely anatase phase TiO₂ and showed an enhanced photocatalytic activity for the degradation of organic pollutant, Reactive Red 141 (RR141), as compared to undoped TiO₂ under visible light irradiation. Photocatalytic mineralization is evaluated by total organic carbon (TOC) analysis. Effect of the concentration of oxidants, namely, potassium peroxomonosulphate (oxone or PMS), potassium peroxodisulphate and hydrogen peroxide, and the amount of catalyst to the dye ratio on the rate of degradation are worked out.

© 2013 Trade Science Inc. - INDIA

KEYWORDS

Sulphur-doped TiO₂;
Fluorine-doped TiO₂;
Reactive Red 141;
Photocatalysis;
Photodegradation of dye.

INTRODUCTION

Photo-induced oxidation and reduction reactions using TiO₂ has received much attention in view of their applications for photochromic sensors^[1] solar cells^[2] and photocatalysis^[3-5]. When TiO₂ is illuminated with light at wavelength < 390 nm, the generation of electron or hole makes it possible to be applied as a photocatalyst. The valence band potential of TiO₂ is positive enough to generate hydroxyl radicals at the surface and the conduction band potential is negative enough to reduce molecular O₂. The hydroxyl radical is a powerful oxidizing agent and attacks organic pollutants at or near the surface of the TiO₂ resulting in complete oxidation of pollutant to CO₂. However, one disadvantage of TiO₂

is that it can only absorb UV light. Therefore, the major aim in the development of TiO₂-based materials is to extend the photoactivity by reducing the bandgap from 3.2 eV towards visible light range in order to utilize solar light more efficiently. One popular approach for TiO₂ modification to red-shift the absorption edge of crystalline TiO₂ is doping transition metals into TiO₂^[6-8]. Although transition metals give the desired red-shift, the photocatalytic activity of metal doped TiO₂ is impaired by thermal instability and an increase in charge-carrier recombination^[8]. Recent research has focused greatly on doping of TiO₂ with non-metal impurities^[9-20] which has been found to be effective in lowering the threshold energy for photochemistry on the TiO₂ surface. It is widely accepted that the dopants such as N, F and C

are incorporated as anions and replace oxygen in the lattice of TiO_2 and effectively extend the light absorption to above 400 nm. The visible light photocatalytic activity of fluorine doped TiO_2 is greater than that of nitrogen doped TiO_2 due to the fact that nitrogen doping creates surface oxygen vacancies while fluorine doping increases surface oxygen vacancies as well as active sites^[21,22]. Ohno et al. reported that S cation-doped TiO_2 powder absorbed visible light more strongly (wavelengths longer than 440 nm) than N, C and the S anion doped TiO_2 powders and showed high photocatalytic activity under visible light^[23]. Liu and Chen also reported that S cation doped TiO_2 effectively photocatalyze the degradation of phenol under visible light^[24]. In the light of the above facts, we planned to prepare fluorine or sulphur doped TiO_2 nanoparticles to effectively utilize visible light for the photocatalytic degradation of azo dyes from wastewaters. In the present work, sulphur or fluorine-doped TiO_2 (S- TiO_2 or F- TiO_2) photocatalysts were prepared by sol-gel technique and the photocatalytic activity of the catalysts were analyzed by observing the mineralization of commercial di-azo dye, Reactive Red 141 (RR141) under visible light illumination.

EXPERIMENTAL

Materials

Analytical grade titanium tetrachloride, thiourea, ammonium fluoride, potassium peroxodisulphate (PDS), hydrogen peroxide (H_2O_2), sodium hydroxide and hydrochloric acid were procured from Merck, India. Potassium peroxomonosulphate (PMS or oxone) ($2\text{KHSO}_5 \cdot \text{KHSO}_4 \cdot \text{K}_2\text{SO}_4$) was obtained from Sigma-Aldrich. Reactive Red 141 ($\text{C}_{52}\text{H}_{34}\text{O}_{26}\text{S}_8\text{Cl}_2\text{N}_{14}$), a di-azo textile dye ($\lambda_{\text{max}} = 543 \text{ nm}$, $\epsilon_{\text{max}} = 25,000 \text{ M}^{-1} \text{ cm}^{-1}$), was obtained from Supra Tulvers, India. Degussa P25 TiO_2 photocatalyst (Degussa, Germany) having a specific surface area of $57 \text{ m}^2 \text{ g}^{-1}$ was used as control.

Preparation of fluorine or sulphur-doped catalyst

Initially, TiCl_4 (0.05 mol) was added drop-wise into 400 mL double distilled water while it was surrounded by an ice bath. After stirring for several minutes, 0.72 mol ammonium fluoride or 0.12 mol thiourea was added

into the above solution and proper stirring was maintained for 30 min. The obtained sol was kept overnight for aging. The precipitate formed was filtered, dried at 343 K, and finally calcined for 3 h at 673 K to obtain the doped TiO_2 photocatalyst. Undoped reference TiO_2 was prepared in the same way but without adding S or F source. The colour of the prepared S-doped and F-doped titanium dioxide powder samples were pale yellow and grey colour, respectively.

Photocatalyst characterization

Powder X-ray diffraction (XRD) patterns of the prepared samples were recorded using a Xpert-Pro diffractometer with $\text{Cu K}\alpha$ radiation ($\lambda = 1.5405 \text{ \AA}$) in the 2θ range of $10\text{--}80^\circ$ at a scan rate of $0.02^\circ \text{ s}^{-1}$. A Shimadzu 2550 UV-visible spectrophotometer equipped with a diffuse reflectance accessory (ISR 2200) was used to obtain the solid-state UV-vis absorption spectra of the catalyst over a range of 300–600 nm.

Photocatalytic activity evaluation

The photodegradation experiments were carried out in a photocatalytic chamber illuminated with three 250 W tungsten-halogen lamps (Philips, India; $\lambda = 360\text{--}2000 \text{ nm}$). The UV radiation ($\lambda < 395 \text{ nm}$) was filtered using a 2 Mil (50 μm thick) CU clear sun-control film (Garware, India) and its transmittance spectrum is given in Figure 1. A known amount of the photocatalyst was added to 70 mL dye solution of desired concentration in a photochemical reactor made of borosilicate glass. The concentration of the dye obtained after mixing the suspension continuously in the dark for 45 min, to ensure adsorption/desorption equilibrium, was used as the initial concentration (C_0) for further kinetic analysis of the photodegradation process. During the irradiation, 5 mL aliquots were withdrawn at appropriate time intervals and the photocatalyst was removed by centrifugation and filtration (0.2 μm). The concentration of the dye was determined spectrophotometrically using a UV-vis spectrophotometer (Shimadzu, 2550) by measuring the absorbance of the clear dye solution at its λ_{max} . The concentration obtained at various irradiation times is denoted as C_t . Total organic carbon (TOC) content of the irradiated samples was measured using TOC analyzer (Shimadzu TOC-V_{CPH} model).

Current Research Paper

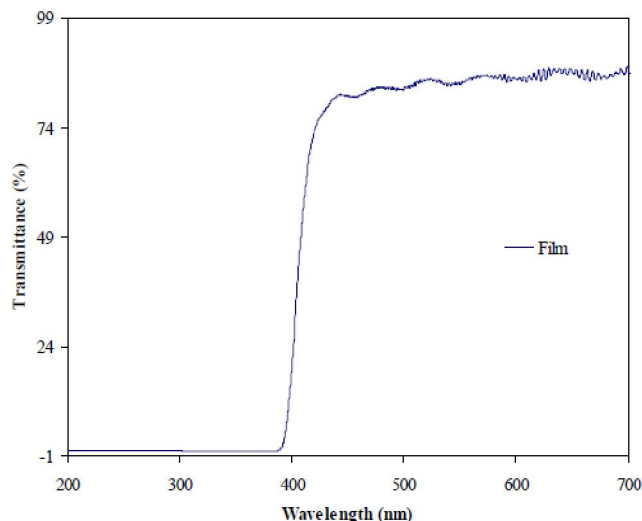


Figure 1 : Transmittance spectrum of 2 Mil CU clear sun-control film (UV filter used).

RESULTS AND DISCUSSION

Crystal phase composition of doped-TiO₂ particles

XRD patterns (Figure 2) confirm that the prepared samples contain only anatase crystallites, as the recorded peaks are corresponding to those indexed for the reflection planes of anatase phase of TiO₂ (JCPDS 21-1272). Anatase phase of TiO₂ is considered to be best photoactive. It is to be mentioned that the Degussa P25 TiO₂ contains anatase and rutile phases (additional peak at $2\theta = 27.61^\circ$ correspond to rutile phase). The XRD peaks of the prepared samples are broader than those of P25 TiO₂ indicating that the crystallite sizes of the prepared catalysts are smaller than that of P25 TiO₂ (~25 nm). The average grain size of the S-TiO₂ and F-TiO₂ crystallites estimated by means of Scherrer equation are 8 and 10.4 nm, respectively. It is to be noted that the samples exhibit the typical structure of TiO₂ crystal without any detectable dopant related peak which may be due to the fact that only some limited amount of dopant might have moved either into the interstitial positions or into the substitutional sites of the TiO₂ crystal structure leading to slight distortions in the peak positions^[25].

Diffuse reflectance spectra

Figure 3 shows the absorption spectra of S-TiO₂ and F-TiO₂ particles together with that of undoped TiO₂ particles. The slight blue shift in the band edge of the

prepared TiO₂ (undoped) compared to P25 TiO₂ indicate that the crystallite size of the TiO₂ prepared in this method is smaller than that of P25 TiO₂, which is in agreement with XRD results. The doped TiO₂ show a clear red shift which can be attributed to the sulphur or fluorine doping. The sulphur doping has extended the range of absorption wavelength towards visible region and has improved the utilization of visible light. This may be due to the substitution of lattice titanium by S⁶⁺ cation that might have formed an isolated narrow band above the valence band of TiO₂ which in turn reduces the bandgap^[15,23,24]. In the case of F-TiO₂, the red shift in optical absorption of TiO₂ was not as it was in S-TiO₂. This indicates that the doped fluorine atoms in TiO₂ particles could not affect the optical absorption property of TiO₂ which was consistent with the result reported by Li et al^[26]. In addition, the colour of sulphur-doped TiO₂ and fluorine doped TiO₂ were pale yellow and grey, respectively. It implied that the doped-TiO₂ absorbs some lower wavelength portion of visible spectrum with low optical absorption intensity^[27].

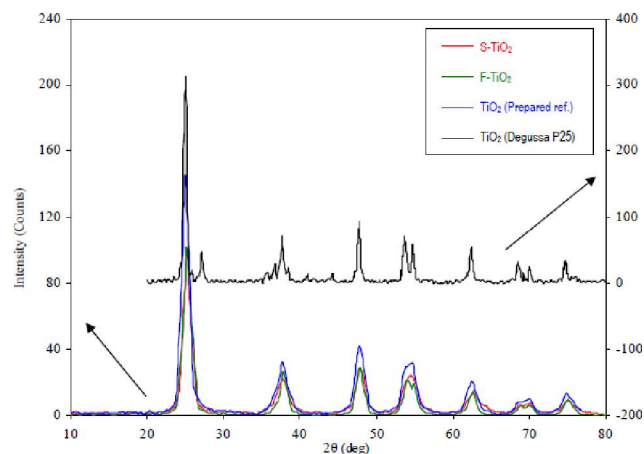


Figure 2 : XRD patterns of S-TiO₂, F-TiO₂, prepared undoped TiO₂ and P25 TiO₂ calcined at 400 °C for 3 h

Photodegradation of RR141

There was no noticeable decolourization of RR141 when the experiments were carried out with (i) dye alone in the dark as well as in light and (ii) dye and catalyst in the dark, which indicated that neither photolysis nor catalysis occurred in this system. However, irradiation of aqueous solutions of the RR141 in the presence of colloidal doped-TiO₂ led to an exponential decrease in the absorption intensity (decrease in concentration) which fit very well in the first-order rate equation as

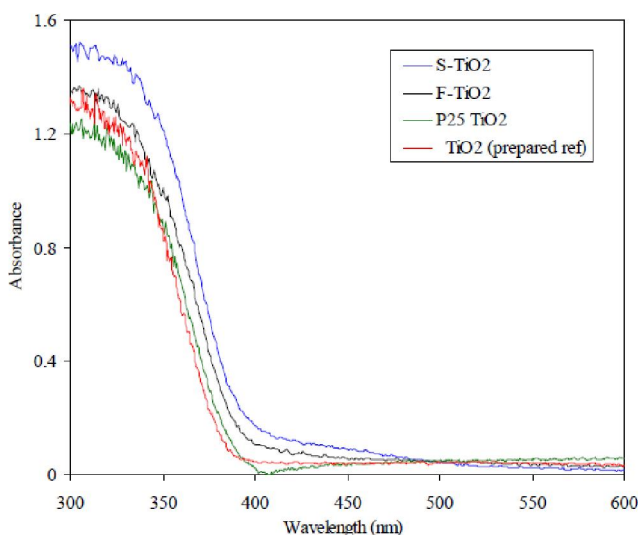


Figure 3: UV-vis absorption spectra of S-TiO₂, F-TiO₂, prepared undoped TiO₂ and P25 TiO₂ calcined at 400 °C for 3 h

shown in Figure 4. Nearly 82 and 79 percent decolourization of 5×10^{-5} M RR141 were attained after 60 min of visible light irradiation in the presence of 1.713 g L^{-1} S-TiO₂ and F-TiO₂, respectively. Under similar experimental conditions, the prepared undoped TiO₂ and Degussa P25 TiO₂ showed only 57 and 46 percent decolourization of RR141 after 60 min irradiation. The slightly higher photocatalytic activity of the prepared TiO₂ compared to Degussa P25 TiO₂ can be attributed to the presence of purely anatase phase in the former while the later contains mixer of anatase and rutile phases. It is clear that the amount of degradation achieved within 60 min using the prepared S-TiO₂ and F-TiO₂ is almost 1.4 times higher than that observed with the bare TiO₂. The higher photocatalytic activities of prepared doped catalysts compared to undoped TiO₂ may be attributed to the synergic effects of absorption in the visible light region (red shift in absorption edge) and increase in the active sites in the modified TiO₂, which increases the electron-hole formation process.

Effect of catalyst concentration on RR141 degradation

The degradation rate was found to increase with the increase in the catalyst concentration initially (Figure 5) and decreases on raising the catalyst amount above the optimum level which is the characteristic of heterogeneous photocatalysis. The optimized catalyst concentration found out for the efficient degradation of RR141 is 1.713 g L^{-1} . The reason for the increase in

the rate of degradation with the increase in the catalyst concentration up to certain level may be due to the increase in the total active surface area which in turn enhance the number of active sites available on the catalyst surface, i.e., the optimum catalyst loading depends on the initial dye concentration as well. When the catalyst concentration is too high, turbidity impedes penetration of light and thereby hampers the photocatalytic activity apparently due to light scattering^[28]. Thus, excess dose of catalyst may not be useful in view of reduced irradiation field as light scattering is prominent.

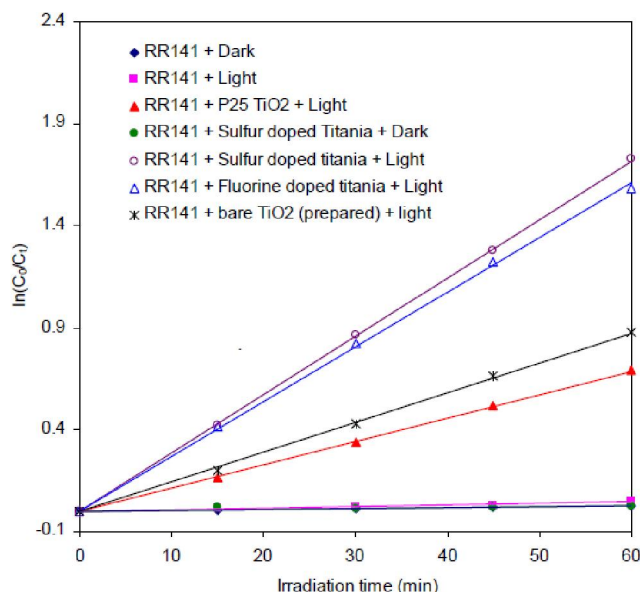


Figure 4 : Normalized concentration vs. time plot for the photocatalyzed degradation of RR141. [TiO₂] = [S-TiO₂] = [F-TiO₂] = 1.713 g L^{-1} ; [RR141] = 5×10^{-5} M

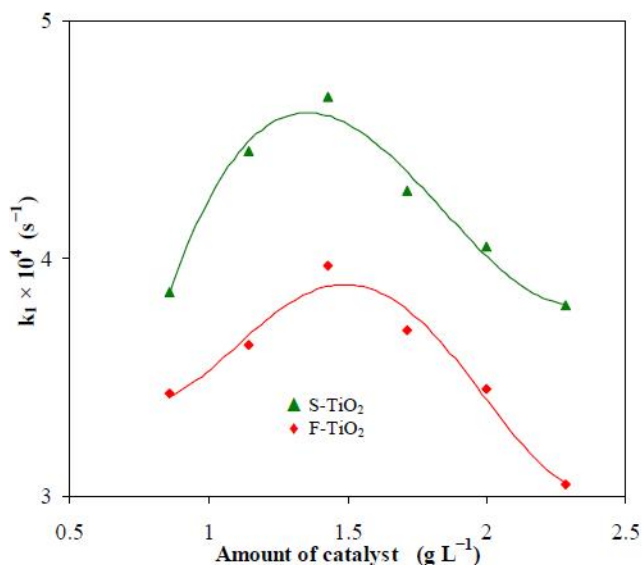


Figure 5 : Effect of catalyst loading on the photodegradation of RR141. [RR141] = 5×10^{-5} M

Current Research Paper

Effect of substrate concentration

It was observed that the degradation of RR141 is reduced with increasing dye concentration (Figure 6). High degradation rate at low dye concentrations may be due to the increase in the reaction between the dye molecules and the oxidizing species (holes or $\cdot\text{OH}$ radicals). Similarly, when the initial concentration of the dye is increased, more dye molecules get adsorbed on the surface of the catalyst creating an inhibitive effect on the reaction between dye molecules and photo-generated holes or hydroxyl radicals. Consequently, with increasing initial dye concentration, the photon flow reaching the catalyst particles will also decrease due to much adsorbed dye molecules^[29]. At elevated dye concentration, dye molecules absorb a significant quantity of light rather than the photocatalyst particles causing a screening effect and reduction in the efficiency of the catalytic reaction. The rate of degradation largely depends on the formation of reactive radicals. Since the intensity of light and catalyst dosage are kept constant with different dye concentration, formation of $\text{O}_2^{\cdot-}$ and $\cdot\text{OH}$ radicals on the surface may decrease with increasing dye concentration as the ratio of catalyst to dye reduces. Therefore, the ratio between the number of available active sites of the catalyst and the number of dye molecules decreases which in turn leads to a multi-layer adsorption of dye in each active site thereby reducing the degradation rate. The noted raise in the degradation rate constant with increasing catalyst to dye ratio (Figure 6 inset) supports this view.

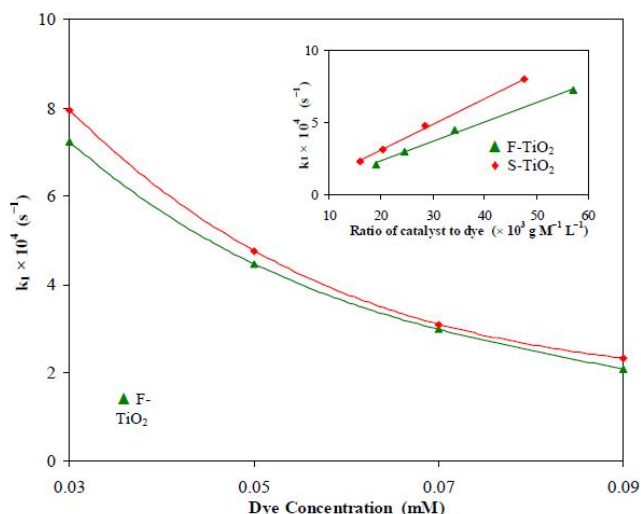


Figure 6 : Rate constants for the photocatalyzed degradation of RR141. $[\text{S-TiO}_2] = [\text{F-TiO}_2] = 1.713 \text{ g L}^{-1}$

The experiments carried out with different dye concentrations (3 to $9 \times 10^{-5} \text{ M}$) and constant catalyst to dye concentration ratio ($C_{\text{doped-TiO}_2}/C_{\text{Dye}} = 2 \times 10^4 \text{ g M}^{-1} \text{ L}^{-1}$) showed that the degradation rate constants are not varying much with dye concentration. The plots of pseudo first-order rate constants vs. dye concentration, when catalyst to dye concentration ratio is $2 \times 10^4 \text{ g M}^{-1} \text{ L}^{-1}$, are given in Figure 7. The degradation rate strongly depends on the ratio of photocatalyst to dye concentration upto 1.5 g L^{-1} of catalyst and above this scattering of light by excess catalyst is dominant which reduces the rate.

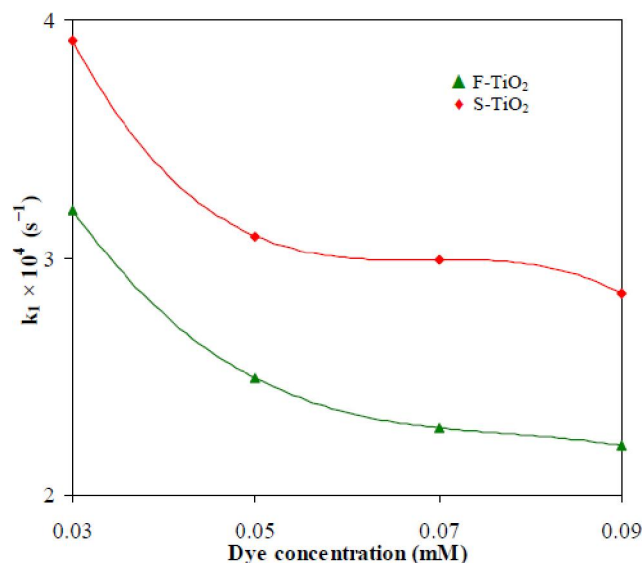


Figure 7 : Plot of rate constant vs. concentration of the dye for the photocatalytic degradation of RR141 at constant doped-TiO₂ to dye ratio ($= 2 \times 10^4 \text{ g M}^{-1} \text{ L}^{-1}$)

Effect of oxidants on photodegradation

Electron scavengers used in photocatalysis retards detrimental electron-hole recombination that occurs at the surface of the catalyst as they capture the conduction band electrons and rapidly dissociate into harmless products and finally form $\cdot\text{OH}$ or other reactive radicals which has the potential to degrade the organic pollutants completely. Oxidants will also increase the oxidation rate of intermediate compounds and avoid the problems caused by low oxygen concentration. The possibility of enhancing the rate of photocatalytic degradation of the chosen dye by the addition of oxidants was scrutinized for three oxidants, namely, PMS (oxone), PDS and H_2O_2 . The preliminary experiment with light and oxidants show $\sim 10\%$ (after 2 h) decolourization of RR141 whereas those experiments

performed in the presence of catalyst and oxidants showed an enhanced decolourization (Figures 8 and 9). Interestingly, the time taken for 95% decolourization is reduced by 5 times on addition of PMS in the photocatalytic degradation of RR141 using S-TiO₂ or F-TiO₂.

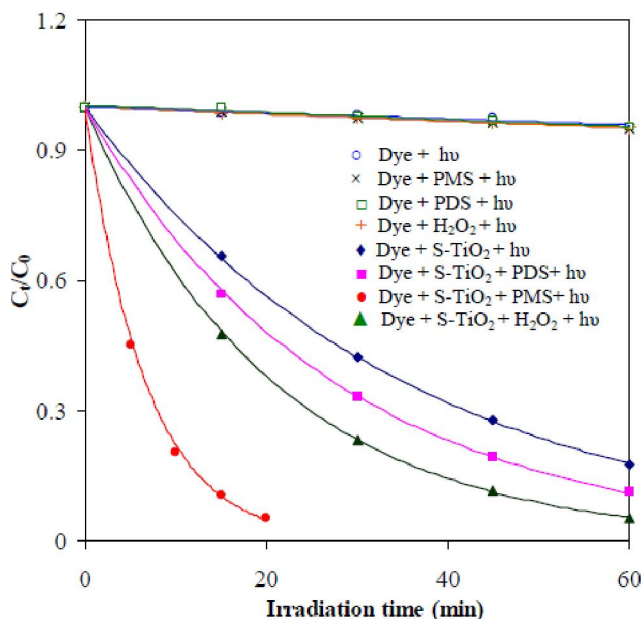


Figure 8 : Experimental data for the photodegradation of RR141 in the presence of oxidants and sulphur-doped TiO₂; $C_{S-TiO_2} = 1.713 \text{ g L}^{-1}$; $C_{RR141} = 5 \times 10^{-5} \text{ M}$; $C_{PMS} = C_{PDS} = C_{H_2O_2} = 2 \text{ mM}$; C_{PMS} , C_{PDS} and $C_{H_2O_2}$ represent the concentration of oxidants used.

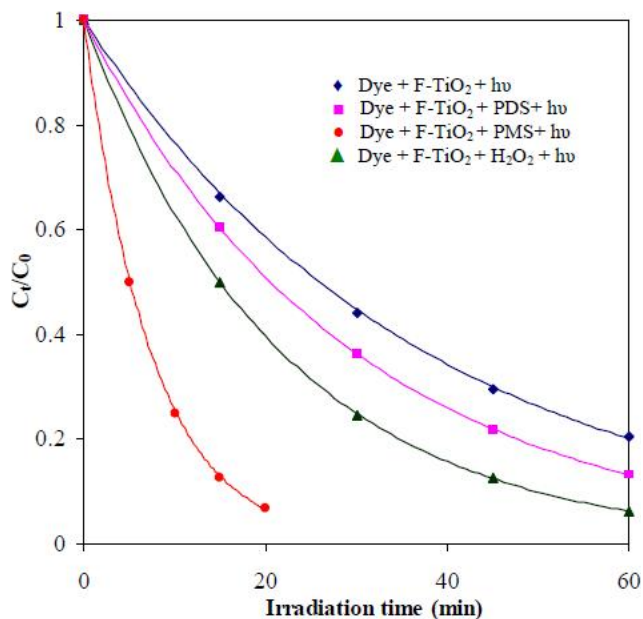


Figure 9 : Experimental data for the photodegradation of RR141 in the presence of oxidants and fluorine-doped TiO₂; $C_{F-TiO_2} = 1.713 \text{ g L}^{-1}$; $C_{RR141} = 5 \times 10^{-5} \text{ M}$; $C_{PMS} = C_{PDS} = C_{H_2O_2} = 2 \text{ mM}$; C_{PMS} , C_{PDS} and $C_{H_2O_2}$ represent the concentration of oxidants used.

It was found that the photocatalytic degradation rates increases initially with increasing concentration and get saturated at 2 mM PMS concentration. The increase in the rate of photodegradation noticed is due to the immediate trapping of photo-generated electrons (e^-) by PMS (electron acceptor) which in turn decreases the recombination of electron-hole pairs thereby enhancing the quantum yield^[30]. In addition, the generation of highly reactive hydroxyl and sulphate radicals during the photocatalytic degradation of PMS assists the photocatalytic degradation of the dye due to the highly oxidizing nature of these radicals. The formation of less reactive radical species $SO_5^{\cdot-}$, by the reactions of $\cdot OH$ and $SO_4^{\cdot-}$ with excess oxone, may be the reason for the decrease in the reaction rate observed when higher concentrations of PMS is used^[28].

Similar to the results obtained with PMS, the photodegradation efficiencies were found to increase initially with increasing amount of persulphate ion or H₂O₂ but tend to decline with further increase in persulphate or H₂O₂ concentration. Present study indicates that 2 mM PDS or H₂O₂ is the optimal concentration to use with S-TiO₂ and F-TiO₂ along with visible light irradiation for the mineralization of RR141. Addition of PDS or H₂O₂ in the photocatalytic degradation of RR141 decreases the time taken for 95% decolourization by 1.5 times. $SO_4^{\cdot-}$ and $\cdot OH$ radicals produced by $S_2O_8^{2-}$ and H₂O₂, respectively, are responsible for the rapid photodegradation of RR141. The $SO_4^{\cdot-}$ radical is a stronger electron scavenger than oxygen^[31] and therefore is expected to enhance photocatalysis efficiency.

Mineralization studies

The complete mineralization of the substrate should be ensured before discharging the wastewater into the ecosystem as the substrate get converted into many intermediate products (during photodegradation) which are sometimes more toxic than the parent compound. Hence, the extent of mineralization of the RR141 was studied by measuring the total organic carbon (TOC) as a function of irradiation time (Figure 10). It is clear from Figure 10 and Figure 8 that, decolourization can be achieved in a short period, whereas, prolonged irradiation is required for the proper mineralization of the parent molecule. It is noted that the doped catalysts

Current Research Paper

have an enhanced mineralization potential under visible light than pure TiO_2 . Also, the extent of photocatalyzed mineralization is always higher when PMS was used as oxidant than PDS and H_2O_2 . The high rate of mineralization achieved while adding PMS can be rationalized by the fact that PMS gets decomposed through both e^-_{CB} and h^+_{VB} of the semiconductor photocatalysts to give $\text{SO}_4^{\cdot-}$ and $\cdot\text{OH}$, whereas H_2O_2 gives only $\cdot\text{OH}$ radicals and PDS gives only sulphate radicals as explained earlier. TOC reduction is much slower than decolourization, suggesting that the breakage of azo bond (chromophore) is the first step of the photocatalytic dye degradation. The relatively slow TOC reduction was most likely caused by the transformation of parent compounds initially into smaller organic intermediates, such as, acetic acids, phenols and aldehydes, which still contribute to the TOC of the solution. The early breakdown products might then undergo further oxidation leading to the production of CO_2 .

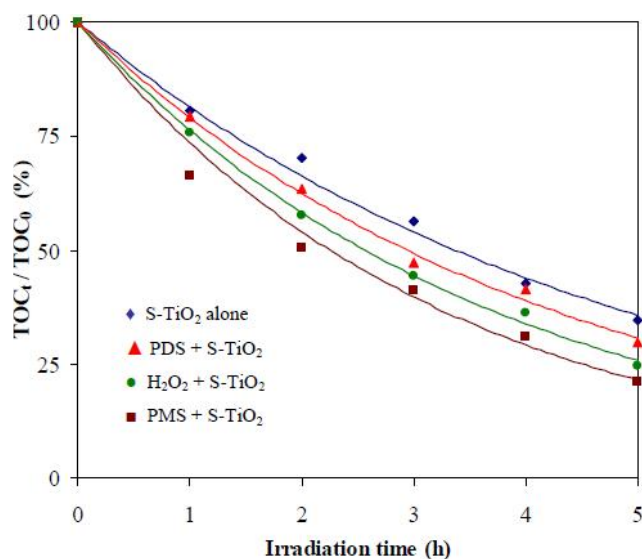


Figure 10 : TOC reduction observed during the photodegradation of RR141 in the presence of S-TiO₂. [S-TiO₂] = 1.713 g L⁻¹; C_{PMS} = C_{PDS} = C_{H₂O₂} = 2 mM; C_{RR141} = 5 × 10⁻⁵ M.

CONCLUSIONS

Purely anatase phase sulphur-doped TiO₂ and fluorine-doped TiO₂ nanoparticles were prepared through sol-gel method. The doped TiO₂ samples showed a red shift in the bandgap absorption. The photodegradation studies confirmed that the amount of

dye degraded within 1 h using the doped samples is 1.4 times higher than that observed with undoped TiO₂ under visible light. The rate of degradation depends on the ratio between the amount of catalyst used and the dye concentration. Almost a 5-fold reduction in the time taken for 95% decolourization of RR141 was observed when PMS was added along with prepared catalyst. PMS is found to be a better choice as an oxidant than conventional hydrogen peroxide or potassium peroxydisulphate and the prepared sulphur-doped TiO₂ have the potential to efficiently remove non-biodegradable di-azo textile dye, RR141, from wastewater streams by utilizing visible portion of solar spectrum.

ACKNOWLEDGEMENTS

The financial support received from the UGC-UPE scheme, Madurai Kamaraj University is gratefully acknowledged.

REFERENCES

- [1] A.Millis, S.L.Hunte; An overview of semiconductor photo-catalysis, *J.Photochem.Photobiol.*, **A108**, 1 (1997).
- [2] M.Gratzel; Photoelectrochemical cells, *Nature*, **414**, 338 (2001).
- [3] H.D.Burrows, M.Canle L., J.A.Santaballa, S.Steenken; Reaction pathways and mechanisms of photodegradation of pesticides, *J.Photochem. Photobiol.*, **B67**, 71 (2002).
- [4] M.R.Hoffmann, S.T.Martin, W.Choi, D.W.Bahne-mann; Environmental applications of semiconductor photocatalysis, *Chem.Rev.*, **95**, 69 (1995).
- [5] H.Y.He; Solvothermal synthesis and photocatalytic activity of S-doped TiO₂ and TiS₂ powders, *Res.Chem.Intermed.*, **36**, 155 (2010).
- [6] M.A.Barakat, H.Schaeffer, G.Hayes, S.Ismat-Shah; Photocatalytic degradation of 2-chlorophenol by Co-doped TiO₂ nanoparticles, *Appl.Catal.*, **B57**, 23 (2004).
- [7] L.Andronic, A.Enesca, C.Vladuta, A.Duta; Photocatalytic activity of cadmium doped TiO₂ films for photocatalytic degradation of dyes, *Chem.Eng.J.*, **152**, 64 (2009).
- [8] M.Sidheswaran, L.L.Tavlarides; Characterization and visible light photocatalytic activity of cerium and iron-doped titanium dioxide sol-gel materials,

Current Research Paper

- Ind.Eng.Chem.Res., **48**, 10292 (2009).
- [9] N.Venkatachalam, A.Vinu, S.Anandan, B.Arabindoo, V.Murugesan; Visible light active photocatalytic degradation of bisphenol-A using nitrogen doped TiO₂, *J.Nanosci.Nanotechnol.*, **6**, 1 (2006).
- [10] S.Yin, H.Yamaki, M.Komatsu, Q.W.Zhang, J.S.Wang, Q.Tang, F.Saito, T.Sato; Low temperature synthesis of TiO_{2-x}N_y powders and films with visible light responsive photocatalytic activity, *J.Mater.Chem.*, **13**, 2996 (2003).
- [11] T.Umebayashi, T.Yamaki, H.Itoh, K.Asai; Bandgap narrowing of titanium dioxide by sulphur doping, *Appl.Phys.Lett.*, **81**, 454 (2002).
- [12] R.Asahi, T.Morikawa, T.Ohwaki, K.Aoki, Y.Tagai; Visible-light photocatalysis in nitrogen-doped titanium oxides, *Science*, **293**, 269 (2001).
- [13] D.B.Hamal, K.J.Klabunde; Synthesis, characterization, and visible light activity of new nanoparticle photocatalysts based on silver, carbon, and sulfur-doped TiO₂, *J.Colloid Inter.Sci.*, **311**, 514 (2007).
- [14] M.Long, W.Cai, H.Chen, J.Xu; Preparation, characterization and photocatalytic activity of visible light driven chlorine-doped TiO₂, *Front.Chem.China*, **2**, 278 (2007).
- [15] H.Znad, Y.Kawase; Synthesis and characterization of S-doped Degussa P25 with application in decolorization of Orange II dye as a model substrate, *J.Mol.Catal.A, Chem.*, **314**, 55 (2009).
- [16] N.Todorova, T.Giannakopoulou, T.Vaimakis, C.Trapalis; Structure tailoring of fluorine-doped TiO₂ nanostructured powders, *Mater.Sci.Eng.*, **B152**, 50 (2008).
- [17] S.Livraghi, K.Elghniji, A.M.Czoska, M.C.Paganini, E.Giamello, M.Ksibi; Nitrogen-doped and nitrogen-fluorine-codoped titanium dioxide, nature and concentration of the photoactive species and their role in determining the photocatalytic activity under visible light, *J.Photochem.Photobiol.*, **A205**, 93 (2009).
- [18] Z.He, L.Xie, J.Tu, S.Song, W.Liu, Z.Liu, J.Fan, Q.Liu, J.Chen; Visible light-induced degradation of phenol over iodine-doped titanium dioxide modified with platinum, role of platinum and the reaction mechanism, *J.Phys.Chem.*, **C114**, 526 (2010).
- [19] M.S.Wong, S.W.Hsu, K.K.Rao, C.P.Kumar; Influence of crystallinity and carbon content on visible light photocatalysis of carbon doped titania thin films, *J.Mole.Catal.A, Chem.*, **279**, 20 (2008).
- [20] H.Wang, J.P.Lewis; Second-generation photocatalytic materials, anion-doped TiO₂, *J.Phys.Condens.Matter*, **18**, 421 (2006).
- [21] D.Li, H.Haneda, S.Hishita, N.Ohashi, N.Labhsetwar; Fluorine-doped TiO₂ powders prepared by spray pyrolysis and their improved photocatalytic activity for decomposition of gas-phase acetaldehyde, *J.Fluorine.Chem.*, **126**, 69 (2005).
- [22] D.Li, N.Ohashi, S.Hishita, T.Kolodiazhnvi, H.Haneda; Origin of visible-light-driven photocatalysis, A comparative study on N/F-doped and N-F-codoped TiO₂ powders by means of experimental characterizations and theoretical calculations, *J.Solid State Chem.*, **178**, 3293 (2005).
- [23] T.Ohno, M.Akiyoshi, T.Umebayashi, K.Asai, T.Mitsui, M.Matsumura; Preparation of S-doped TiO₂ photocatalysts and their photocatalytic activities under visible light, *Appl.Catal.*, **A265**, 115 (2004).
- [24] S.Liu, X.Chen; Visible light response TiO₂ photocatalyst realized by cationic S-doping and its application for phenol degradation, *J.Hazard.Mater.*, **152**, 48 (2007).
- [25] W.L.Kostedt, A.A.Ismail, D.W.Mazyck; Impact of heat treatment and composition of ZnO-TiO₂ nanoparticles for photocatalytic oxidation of an azo dye, *Ind.Eng.Chem.Res.*, **47**, 1483 (2008).
- [26] D.Li, H.Haneda, S.Hishita, N.Ohashi; Visible-light-driven N-F-Co doped TiO₂ photocatalysts, 2, Optical characterization, photocatalysis and potential application to air purification, *Chem.Mater.*, **17**, 2596 (2005).
- [27] H.L.Qin, G.B.Gu, S.Liu; Preparation of nitrogen-doped titania with visible-light activity and its application, *C.R.Chimie*, **11**, 95 (2008).
- [28] J.Madhavan, B.Muthuraaman, S.Murugesan, S.Anandan, P.Maruthamuthu; Peroxomonosulphate, an efficient oxidant for the photocatalysed degradation of a textile dye, acid red 88, *Sol.Energy Mater.Sol.Cells*, **90**, 1875 (2006).
- [29] N.Daneshvar, D.Salari, A.R.Khataee; Photocatalytic degradation of azo dye acid red 14 in water, investigation of the effect of operational parameters, *J.Photochem.Photobiol.*, **A157**, 111 (2003).
- [30] S.K.Kuriechen, S.Murugesan, S.P.Raj, P.Maruthamuthu; Visible light assisted photocatalytic mineralization of Reactive Red 180 using colloidal TiO₂ and oxone, *Chem.Eng.J.*, **174**, 530 (2011).
- [31] J.T.Jung, J.O.Kim, J.Y.Choi; Effect of various oxidants in a photocatalysis/filtration system for the treatment of contaminants, *Res.Chem.Intermed.*, **35**, 243 (2009).